

A DETECTOR SYSTEM FOR COSMIC RAY ELECTRONS*

D. HOVESTADT†, P. MEYER+ and P. J. SCHMIDT§

Enrico Fermi Institute, The University of Chicago, U.S.A.

Received 22 April 1970

The construction, operation and calibration of a balloon-borne counter telescope is described. The instrument is designed for a measurement of cosmic ray electrons in the energy range from 15 MeV to 15 GeV. Results of calibrations on electron accelerators for energies between 10 MeV and 6 GeV are compared with

predictions from shower theory. The detector has an energy resolution between 20 and 40 percent for electrons and discriminates efficiently against protons. The geometry factor is $18 \text{ cm}^2 \text{ sterad}$

1. Introduction

Over the past nine years a major effort has been devoted at the University of Chicago toward measuring the energy spectrum of primary cosmic ray electrons and positrons. Considerable development in detector systems has taken place aimed at achieving unique particle discrimination and identification over a wide range of energies as well as good energy resolution. As a result of this work we have recently designed and constructed a balloon-borne instrument which fulfills the above requirements to a high degree. This instrument has been used for measurements of the electron spectrum in the years of 1968 and 1969. A total of five balloon flights were carried out during the summer months from Ft. Churchill, Manitoba. It is scheduled for additional measurements in the coming years in order to investigate long-term time variations of the electron energy spectrum.

Our experience with this instrument in calibration runs as well as during flights has shown that it yields excellent results over a range of electron energies from about 15 MeV to 15 GeV. It has a reasonably large geometry factor of $18 \text{ cm}^2 \text{ sterad}$ which enables one to obtain energy spectra with good statistical accuracy in spite of the low primary electron flux¹⁾, and to study in detail the short term intensity variations which are associated with the diurnal changes of the geomagnetic cut-off at high magnetic latitudes²⁾.

Since we believe that knowledge of the features of this instrument is likely to be useful to other investigators in this field of research and is essential for a critical evaluation of our results, we wish in this paper to discuss the detector system in some detail and to describe its characteristics and capabilities.

* Work supported in part by the National Science Foundation under grants No. GA-1277 and GA 17210.

† Permanent address, Max-Planck-Institut für Extraterrestrische Physik, Garching, Germany.

+ Also Department of Physics.

§ NSF Trainee 1965-1969

2. The detector system

2.1. OVER-ALL DESCRIPTION OF THE INSTRUMENT

At the outset, it should be kept in mind that our instrument is designed for measurements at balloon altitudes and, in order to reduce the contribution by secondary particles produced in the residual overlying atmosphere, we must attempt to reach as high an altitude as possible. This requirement puts constraints on the permissible mass of the detector system and to some extent on its size. The isotropic incidence of particles requires good directional discrimination and

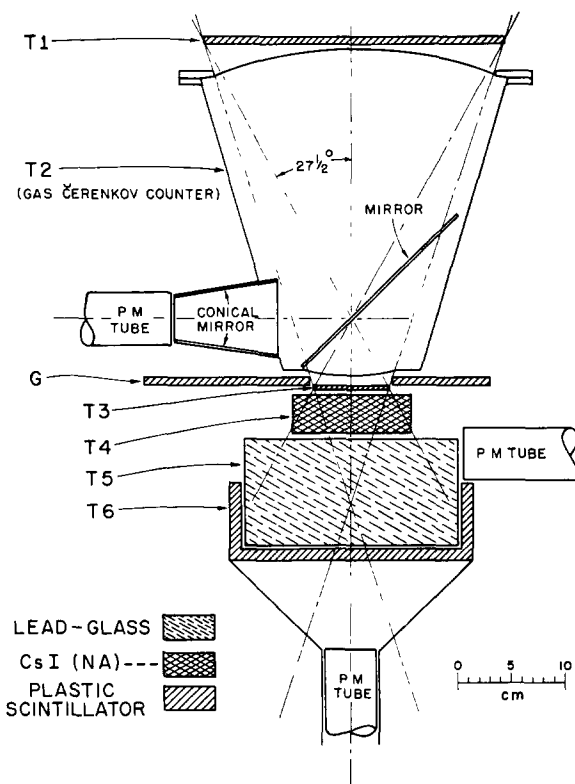


Fig. 1. Schematic cross section of the detector system.

the abundant flux of low energy primary and secondary nuclear particles has to be eliminated.

A schematic cross section of the instrument is shown in fig. 1. It consists of a counter telescope made of NE 102 A plastic scintillators, a CsI(Tl) scintillator, a gas Čerenkov counter, a lead glass Čerenkov counter, and a plastic penetration counter. The maximum angle of acceptance is 27.5° from vertical, and the geometry factor is $18 \text{ cm}^2 \text{ sterad}$, defined by the two plastic scintillators T1 and T3. These two counters have diameters of 28 cm and 7 cm and thicknesses of 0.5 cm and 0.32 cm respectively. The gas Čerenkov counter T2 is filled with Freon 12 at 2.5 atm pressure and rejects all particles with $\gamma = E/mc^2 \leq 13.5$. The T1, T2, T3 coincidence is used to initiate the measuring process for each event.

Located under this telescope are a CsI counter (T4) of a thickness corresponding to 2 radiation lengths and a lead glass Čerenkov counter (T5), 6.7 radiation lengths thick. Particles entering the telescope are either absorbed or, together with their secondaries, penetrate the plastic cup counter T6.

The reason for introducing two separate counters T4 and T5 is twofold:

1. this separation permits distinguishing electrons from interacting protons at high energies, and
2. counter T4 provides good energy resolution for electrons at low energies.

The output of counter T6 serves as an additional parameter for energy determination in those cases where the energy of the initiating electron is sufficiently high that the shower penetrates T5. The output from T6 yields the number of penetrating shower particles.

The addition of a guard counter G, whose firing in coincidence with the master pulse T1 T2 T3 is indicated, serves to identify events which are triggered by showers initiated above and around the apparatus. It also rejects events in which secondary particles strike the window of the gas counter photomultiplier leading to a false triggering of T2 by Čerenkov light produced in the window material.

For each event, pulse heights are measured from counters T3, T4, T5 and T6 by 256 channel analyzers. The pulse height in T3 indicates whether a singly charged relativistic particle has initiated the event, and the information from the other pulse heights are used for energy determination as well as discrimination against events which are not due to an incoming electron.

All count rates of individual counters as well as the rates of twofold coincidences T1 T3 and threefold coincidences T1 T2 T3 are monitored for a continuous

performance check of the instrument and to determine the dead time of the system introduced by the pulse-height analysis process. The information on rates and pulse heights is digitized by the electronics system and recorded by an on-board magnetic tape recorder as well as telemetered to the ground.

The entire system is housed in an aluminum shell and kept under atmospheric pressure during the balloon flights. The amount of material in front of counter T4 in the acceptance cone is 2.2 g/cm^2 of aluminum, plastic and Freon 12 or < 0.1 radiation lengths. This includes the telescope counter and aluminum shell and corresponds to a total energy loss of about 4 MeV for all incident electrons with energies above 7 MeV. The weight of the instrument in its shell and including batteries amounts to approximately 400 lb..

2.2. THE GAS ČERENKOV COUNTER

This device consists of a conical container filled with Freon 12 to an absolute pressure of 2.5 kg/cm^2 at 20°C which leads to an index of refraction $n-1 = 2.8 \times 10^{-3}$. A thin flat mirror of lucite with evaporated aluminum coat is placed in the pressure vessel at a 45° angle to reflect the Čerenkov light toward a 2" photomultiplier (Type EMI 9635 QA) with quartz window*. Further collimation of the light is achieved by using a conical mirror in front of the photomultiplier (see fig. 1). The angle of the light collecting cone is so chosen that light emitted from a relativistic particle arriving within the telescope aperture is seldom reflected more than three times before reaching the photomultiplier surface. Those reflections have been taken into account when estimating the light collection efficiency.

For an estimate of the number of photo-electrons produced by a particle which penetrates the Čerenkov counter we use the expression given by Jelley³⁾

$$\frac{dN}{dl} = 2\pi\alpha\xi\eta_0 \left(1 - \frac{1}{n^2\beta^2}\right) \int_{\lambda_1}^{\infty} \frac{S(\lambda)}{\lambda^2} d\lambda,$$

where $\alpha = 1/137$; ξ = light collection efficiency which we estimate to be 25% or higher; $\eta = \eta_0 S(\lambda)$ the quantum efficiency of the photomultiplier tube ($\eta_0 \approx 28\%$ for EMI 9635QA) and n = index of refraction of the gas. Evaluating this expression using the known frequency response of the photomultiplier and an ultraviolet cut-off wavelength $\lambda_1 = 2100 \text{ \AA}$ due to

* Several instances of fractured quartz windows have led us to more recently replace this multiplier by an RCA C31000 C with a window of 9741 glass

absorption in Freon 12 leads to about 0.4 photoelectrons produced for each cm pathlength in the gas by a highly relativistic particle. Since the average pathlength is about 25 cm, one expects roughly 10 photoelectrons per relativistic particle.

Fig. 2 shows the efficiency of the gas counter as a function of γ for different high energy limiting values of the number of photoelectrons produced. A Poisson distribution of the number of electrons emitted at the cathode and first two dynodes is assumed. Experimental data obtained with beams of electrons at different energies are also shown in this figure.

2.3. THE CSI COUNTER AND THE LEAD GLASS ČERENKOV COUNTER

The combined Csl scintillation counter (T4) and lead glass Čerenkov counter (T5) are the elements used for energy determination of the incident particles.

We first briefly describe the construction of these counters. The Csl crystal with a diameter of 11.2 cm and a thickness of 3.5 cm, corresponding to two radiation lengths, is housed in an aluminum container, coated with a highly reflecting white paint. It is viewed from the side by an RCA 7767 photomultiplier ($\frac{3}{4}$ " photocathode). The lead glass Čerenkov counter has a diameter of 20 cm and thickness of 10.2 cm. It consists of Schott SF6FA glass (density 5.19 g/cm², index of refraction $n = 1.805$) and therefore represents 6.7 radiation lengths. It is also mounted in an aluminum container with highly reflecting white walls. Three photomultipliers (RCA 2063) are optically coupled to the upper edge of the lead glass (see fig. 1). In order to match the outputs of the three tubes, a chip of a

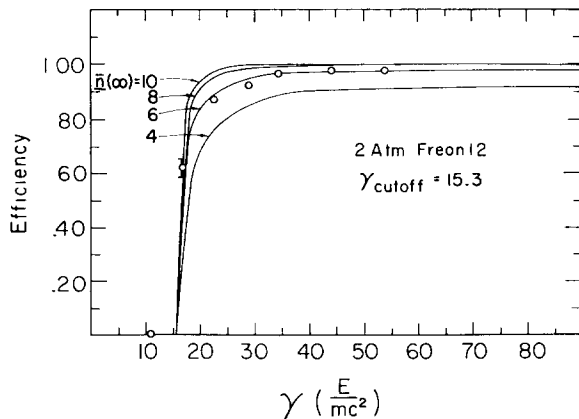


Fig. 2. Efficiency of the gas Čerenkov counter as a function of γ . Solid curves calculated for an average of 4, 6, 8 and 10 photoelectrons at very high γ . (Note that these data were calculated and measured for a Freon 12 gas pressure of 2 atm.).

CsI and an ^{241}Am α -particle source are placed in the bottom center of the lead glass. The light from this scintillator, which is in a symmetric position with respect to the three photomultiplier tubes is used to insure identical gain of the three tubes and preamplifiers.

The combined light outputs from the CsI crystal and the lead glass Čerenkov counter are used to determine the energy of an electron incident at T4. If this energy is E_0 we may write

$$E_0 = \alpha \cdot (T4) + \beta \cdot (T5) + L(E_0), \quad (1)$$

where (T4) and (T5) stand for the pulse heights of the two counters and $L(E_0)$ is the part of the energy in the electron-photon shower which escapes, due to the limited size of the counter system. The coefficients α and β relate the pulse height to the energy deposited in each counter. In order to determine the energy of an incoming electron from the pulse heights in T4 and T5 the coefficients α and β have to be known.

The energy responses of the Csl scintillation counter and the lead glass Čerenkov counter are somewhat different. To a very good approximation it can be assumed that the shower energy is exclusively dissipated by the ionization losses of shower electrons. Since the light output in the Csl detector – at least for electrons and singly charged relativistic particles – is proportional to the ionization, the light output of T4 is directly proportional to the dissipated energy. Pulse heights therefore can be related to the ionization loss by observing penetrating cosmic ray μ -mesons at sea level. The average energy loss of μ -mesons above the gas Čerenkov counter threshold ($\gamma = 13.5$) has been obtained by folding the sea level muon energy

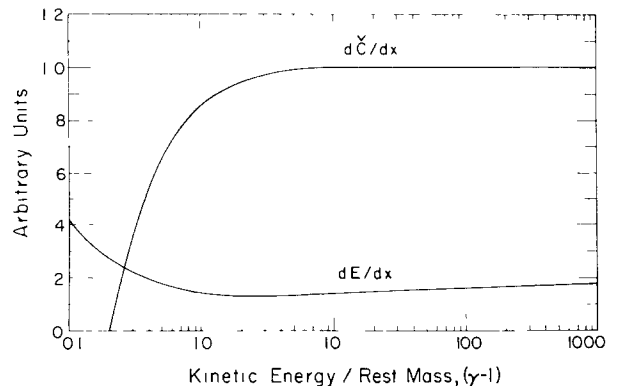


Fig. 3. Comparison of Čerenkov light output and energy loss by ionization as a function of kinetic energy in lead glass (Schott SF 6 FA).

spectrum⁴⁾ with the values for the energy loss given by Barkas and Berger⁵⁾ and by Trower⁶⁾. Also taking into account the pathlength distribution of muons in the counter, the average energy loss is found to be 26.5 MeV for counter T4. Using the experimental pulse height distribution one finds the ratio of the most probable energy loss to the average energy loss to be 0.83, in rough agreement with calculations for the energy loss distribution. Thus, the energy corresponding to the peak of the muon pulseheight distribution is 22.1 MeV and the coefficient α can be determined.

In the case of the lead glass Čerenkov counter the proportionality of the light output with the dissipated shower energy is not that obvious. This can be seen from fig. 3 where we have plotted both the relative light yield and the energy loss as a function of electron energy for the lead glass counter. While the Čerenkov light output reaches an asymptotic value with increasing energy, the energy loss continues to increase up to very high energies. The output of the Čerenkov counter is therefore proportional to the total pathlength of shower particles rather than to the dissipated energy. However, for a thick counter the main contribution to the total path length comes from particles near and beyond the shower maximum. As a consequence of the similarity rules of shower theory⁷⁾ the energy spectrum of shower electrons in this region is nearly independent of the primary electron energy and an almost linear response of the Čerenkov counter output with energy is also expected. It follows, therefore, that β is also nearly independent of energy. A rough value of β can be obtained from observation of the light output by penetrating muons, which lose, on the average, 88 MeV in the lead glass. This leads to $\beta = 12.6 \text{ MeV}/X_0$. A direct calibration of the counter with monoenergetic electrons is necessary if one wishes to determine β with higher accuracy, since its value depends on the details of the construction of the counter and is sensitive to the cut-off energy.

In order to determine β from calibration runs, the term $L(E_0)$ of eq. (1) has to be known. $L(E_0)$ can be calculated from shower theory and, once β is determined, eq. (1) can be used to extrapolate beyond the highest calibration energy (5.7 GeV).

The function $L(E_0)$ is obtained from recent Monte Carlo calculations by Nagel⁸⁾ and by Voelkel⁹⁾. Using the work of Kantz and Hofstadter¹⁰⁾, these authors calculate the fraction of total shower energy which is dissipated in a cylindrical, ring-shaped element of radial width Δr and depth Δt in an infinite absorber. By integrating the fractional energy loss over a region which corresponds to the dimensions of our counter

system ($r = 8 X_0$, $t = 8.7 X_0$), one obtains the energy containment factor $c(E_0) = 1 - l(E_0)$. $l(E_0)$ is the relative energy loss factor and is related to $L(E_0)$ by $L(E_0) = l(E_0) E_0$.

The calculations by Nagel and Voelkel were made for lead and copper absorbers at various energies up to 6 GeV. In fig. 4, we show the calculated energy containment factors $c(E_0)$ together with three experimental points taken at 185 MeV by Kantz and Hof-

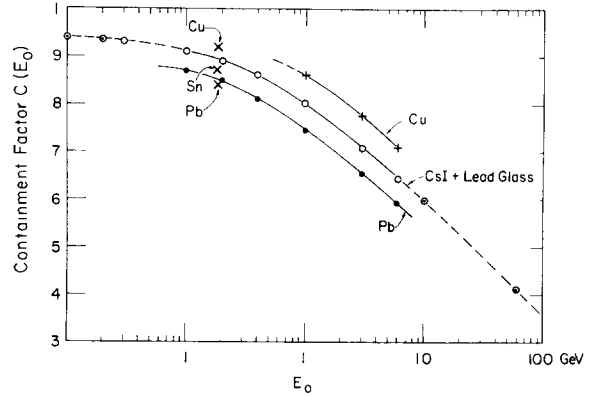


Fig. 4 The energy containment factor for electron showers in copper, lead and the CsI-lead glass counter combination used in this experiment as a function of the energy of an incident electron + Monte Carlo calculation for 9 radiation lengths of copper⁹⁾, ● Monte Carlo calculation for 9 radiation lengths of lead^{8,9,11)}, × experimental results¹⁰⁾, ○ interpolation and ○ extrapolation for 8.7 radiation lengths of combined CsI and lead glass counters

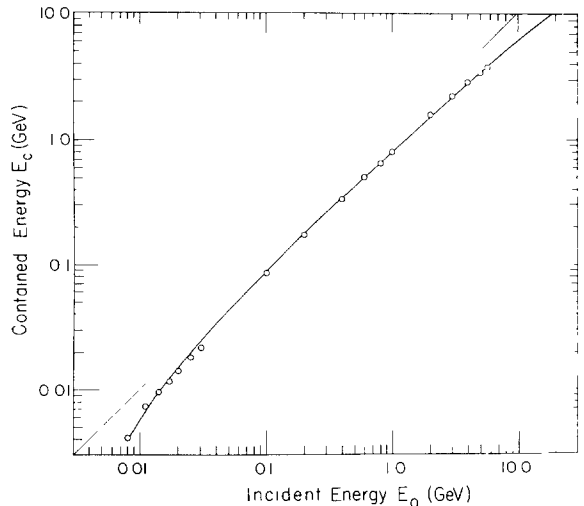


Fig. 5. Calculated contained energy $E_c = E_0 - L(E_0) - 4 \text{ MeV}$ as a function of the incident energy E_0 . The experimental points were obtained from accelerator calibrations with the parameter β [see eq. (3)] adjusted for best fit. The light line, shown for comparison, represents $E_c = E_0$.

stadter¹⁰) for lead, tin and copper. Also shown in fig. 4 is the linear interpolation which represents the curve applicable to our detector system T4 and T5

The extrapolation of the containment factor to energies below 100 MeV was made under the following assumptions:

1. The tail of the shower curve in an infinitely thick absorber follows an exponential, $\exp[-\lambda_{\min} t]$, beyond $8.7 X_0$.

2. The tail of the normalized shower curve shifts in depth t by the same amount as the position of the shower maximum $t_{\max}(E_0)$ when the energy E_0 is varied. Here λ_{\min} is the minimum linear absorption coefficient per radiation length for bremsstrahlung¹²). With these assumptions, the energy dependence of the loss factor is roughly

$$l(E_0, t) = l(E_1, t) \exp \{-\lambda_{\min} [t_{\max}(E_1) - t_{\max}(E_0)]\}.$$

Using $l(E_1, t)$ at $E_1 = 100$ MeV from Nagel, $\lambda_{\min} = 0.24 X_0^{-1}$ and the interpolation formula⁸)

$$t_{\max}(E_0, E) = 1.11 \log E_0 - 0.25 \log E - 3.87 \quad (E \text{ in MeV}), \quad (2)$$

one obtains the extrapolation for the containment factor that is shown in fig. 4. E is the cut-off energy as defined by shower theory. The extrapolation to energies above 6 GeV is discussed in section 2.4.

To obtain the contained energy E_c as a function of E_0 one has to consider in addition to $L(E_0)$ the energy loss of the incident particles prior to reaching counter T4. This amounts to about 4 MeV and is independent of energy. The solid line in fig. 5 shows the calculated contained energy vs incident energy:

$$E_c = \alpha \cdot (T4) + \beta \cdot (T5) = E_0 - L(E_0) - 4 \text{ MeV}. \quad (3)$$

Experimental points, which were obtained from calibrations with monoenergetic electrons (see section 3) are included using the best fit for a constant value of β . The fit is excellent over 3 decades in energy and yields $\beta = 13.4 \text{ MeV}/X_0$. This is in good agreement with Nagel's calculations for a cut-off energy of 150 keV.

2.4. THE PENETRATION COUNTER

The penetration counter T6 consists of a cup-shaped plastic scintillator, made of NE102A scintillation material and is viewed by an RCA 2063 photomultiplier through a light funnel coated with a highly reflectant white paint. For each event which triggers the counter telescope the pulse height of counter T6 is analyzed.

The T6 counter serves several purposes:

1. This counter determines whether any charged particles are emerging from the lead glass counter T5. Its shape insures that very few penetrating particles can miss it.
2. It helps one to distinguish energetic electrons from protons.
3. At higher energies it provides an independent determination of electron energy since it measures the number of escaping electrons.

Direct calibrations of the instrument have been made with monoenergetic electron beams with energies up to 5.7 GeV. Therefore one has to rely on shower theory to extrapolate the number of particles penetrating into T6 to higher energies. These extrapolations make extensive use of the Monte Carlo calculations by Nagel⁸) and by Voelkel⁹).

In particular, the extrapolation is based on the following assumptions:

1. The shape of a shower is independent of E_0 , if the unit of depth is chosen to be t_{\max} and the unit for the number of electrons is chosen to the maximum number π_{\max} .

2. The number of electrons in the shower maximum $\pi_{\max}(E_0, E)$ is correctly given by the expression⁹)

$$\pi_{\max} = 0.08 \frac{E_0 + 37.5}{E + 12.8} + 0.45 \quad (E \text{ in MeV})$$

up to the highest energies which we consider. This expression has only been verified to 6 GeV.

3. Eq. (2) of the preceding paragraph for the depth of the shower maximum $t_{\max}(E_0, E)$ is valid beyond 6 GeV.

A general justification for these assumptions follows from shower theory [see Rossi¹³), Ott⁷)]. Their application leads to the number of escaping electrons π_0 which traverse the penetration counter at the depth of our counter system of $t_0 = 8.7 X_0$:

$$\pi_0(E_0, E, t_0) = A(E_0, E, t_0) \pi_{\max}(E_0, E),$$

where

$$A(E_0, E, t_0) = \frac{\pi_0(E_0, E, t_0)}{\pi_{\max}(E_0, E)} = \frac{\pi(6 \text{ GeV}, E, t_x)}{\pi_{\max}(6 \text{ GeV}, E)}$$

and

$$t_x = t_0 \frac{t_{\max}(6 \text{ GeV}, E)}{t_{\max}(E_0, E)}.$$

Fig. 6 shows the position of the shower maximum in lead according to expression (2) as well as the ratio A as a function of E_0 with $t_0 = 8.7 X_0$ and $E = 2.5 \text{ MeV}$

for the plastic scintillation material used in the penetration counter T6.

The average number of electrons escaping the T4 and T5 assembly, π_0 , as a function of E_0 is shown in fig. 7 together with results from calibration runs for this and another experiment from this laboratory. For comparison $\pi_{\max}(E_0)$ is also plotted.

A similar procedure is used to extrapolate the shower energy left in T4 and T5, using the energy containment factor $c(E_0, E, t_x)$ as calculated by Voelkel⁹⁾ for $E_0 = 6$ GeV with $E \approx 150$ keV, appropriate for lead glass. It should be noted that the extrapolation of the energy containment factor to high energies is probably

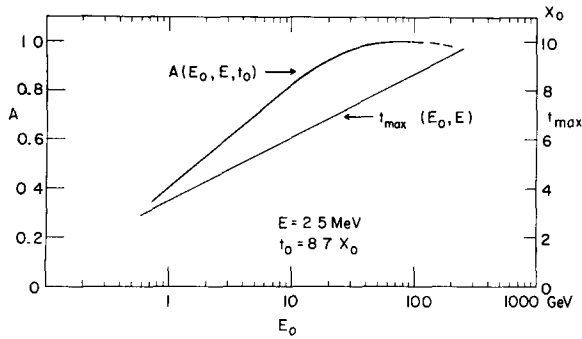


Fig. 6 Position of the shower maximum t_{\max} in lead as a function of incident electron energy and the ratio A of the number of electrons escaping to the number at the shower maximum for a counter of 8.7 radiation lengths depth as a function of the incident electron energy.

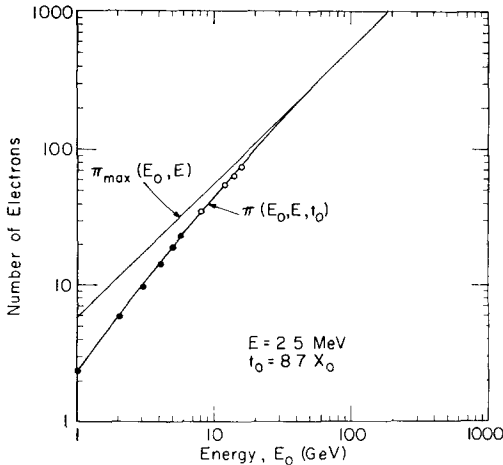


Fig. 7. Calculated maximum number of shower electrons π_{\max} as a function of incident electron energy E_0 and calculated number of electrons π present at a depth of 8.7 radiation lengths, corresponding to the thickness of the CsI-lead glass counter combination. The points represent the average number of electrons at this depth as measured by accelerator calibrations. \circ Fanselow and Hartman¹⁴⁾.

less reliable than the extrapolation of the number of escaping electrons since the latter depends less sensitively on the knowledge of the critical energy of the material. For electron energies beyond 10 GeV we have therefore used mainly the output from the penetration counter to determine the electron energy.

3. Particle identification and calibration

3.1. ELIMINATION OF PROTONS AND BACKGROUND

To produce a reliable measurement of the flux and energy spectrum of primary electrons, the instrument must be capable of identifying individual electrons which traverse its aperture with high efficiency and it must be immune to contaminations by interacting protons masquerading as electron showers.

Our procedure for efficient elimination against proton contamination has been to impose severe criteria for the pulse height pattern to be followed by each event. As a result of these criteria a fraction of electron events will also be eliminated from the analysis. This fraction, however, is accurately known as a function of energy from calibrations with mono-energetic beams of electrons over a range of energies from 8 MeV to 6 GeV. Beyond that energy we have to extrapolate at the present*.

We shall now describe this procedure in more detail. Initial screening is provided by the threefold coincidence (T1 T2 T3) which initiates an event. The presence of the gas Čerenkov counter T2 in the telescope insures that the initiating particle is moving downward and has a $\gamma > 13.5$. It is further required that the pulse height in counter T3 corresponds to a minimum ionizing, singly charged particle within rather narrow limits. These two criteria require a knowledge of the gas counter efficiency ($\approx 98\%$) and the pulse height distribution in T3 for electrons at various energies. Both quantities are obtained from calibration runs.

The guard counter G may be fired by a shower initiated in the atmosphere above and around the equipment or by a secondary particle resulting from an interaction in T4 or T5 and which is capable of firing T2 by Čerenkov light produced in the face of its phototube, etc. All events which fire counter G are discarded from the analysis and again the calibration runs are used to obtain the fraction of electrons which, at each energy, is eliminated in this process.

All events which survive the above screening procedure are sorted according to the pulse height pattern

* Calibrations with electrons up to 15 GeV have recently been carried out, and confirm our extrapolation.

which they exhibit in counters T4, T5 and T6. This "tagging" procedure which puts the events in one of 27 groups is illustrated schematically in fig. 8. The tag 0, 1 or 2 is applied depending on whether the light output is below, around or above the peak for minimum ionization loss. Also shown in fig. 8 are the groups into which most of the electrons and protons fall.

This particle identification method is not 100% efficient. Statistical fluctuations in the electron shower development, and in the particle energy loss together with the finite counter resolution prevent the tagging from being entirely correct. The efficiency with which electrons are identified must therefore be determined experimentally by calibration runs in which the incoming particle is known to be an electron of specified energy and direction.

The removal of the proton contamination is the most important problem. Even with a Čerenkov counter cut-off of 13.5 GeV, the number of protons capable of triggering the apparatus is roughly the same as that of electrons. High energy nuclear cross sections¹⁵⁾ indicate that about 65% of the protons will not suffer an interaction while traversing the detector system, therefore showing minimum ionization in all counters and being properly tagged. The remainder will interact in either T4 or T5 and, from that point on, produce pulse heights different from a minimum ionizing particle. The majority of interactions takes place in T5. These events will therefore be properly tagged since the pulse height in T4 still corresponds to a minimum ionizing particle. In order to eliminate the protons which interact in T4 we have computed the ratio of the number of T4 interactions to the number of T5 interactions. This ratio can be readily obtained

from the knowledge of the cross sections and the amount of material contained in these counters. One now further assumes that the contained energy $E_c = \alpha \cdot (T4) + \beta \cdot (T5)$ is the same, no matter whether the proton has interacted in T4 or T5. Then, multiplying the known "spectrum" of proton interactions in T5 by the ratio T4/T5 will yield the number of T4 interactions as a function of E_c . This method leads to corrections of no more than 10% at all electron energies.

An independent check of this method has been used by applying an entirely different technique. Balloon flight data show that, if events are displayed in a two-dimensional array of T5 vs T6 output, the majority of events due to interacting protons lie on a different "track" than electron showers. As is qualitatively expected, the (T5)/(T6) pulse height ratio is considerably larger for electron showers than for proton interactions. This separation of electrons and proton events can be used to eliminate most of the protons. It introduces a small loss of electrons, which however can be corrected for with the help of the electron calibration data.

3.2. CALIBRATION

To obtain an energy calibration as well as the efficiency of detecting electrons at various energies under the criteria discussed above, a series of measurements was made using beams from electron accelerators. In the energy range from 8 to 30 MeV we were able to use the linear accelerator at the Argonne Cancer Research Hospital, University of Chicago, the range from 100 MeV to 1 GeV could be covered with the synchrotron of the Cornell University Laboratory for Nuclear Studies, and 1 GeV to 5.6 GeV electrons were available to us at the Cambridge Electron Accelerator*.

The first requirement for the calibration is the determination of the quantity β in the expression for the total contained energy $E_c = \alpha \cdot (T4) + \beta \cdot (T5)$. In 2.3 we have described the method by which β is obtained. We refer again to fig. 5 in which E_c is plotted against the energy of the incident electron. The close agreement of this one-parameter fit with the data over almost three decades is the justification for the assumption that β is energy independent and that the proper form of $L(E_0)$ was used.

One may independently check that the value of β is correct by studying the energy resolution of the

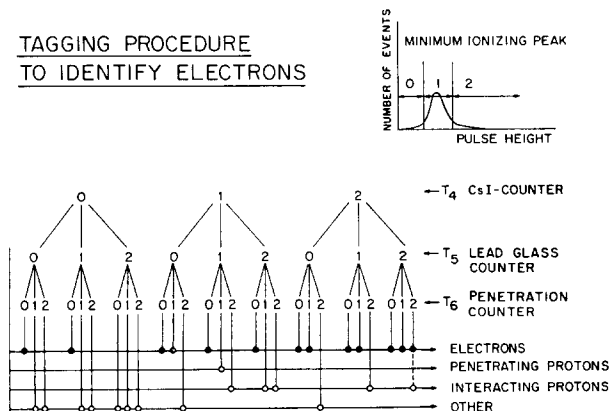


Fig. 8 Schematic diagram of the tagging procedure employed to identify incident particles as electrons.

* We are grateful to Dr. L. Skaggs of the University of Chicago, Dr. J. Rouse of Cornell University and Dr. K. Strauch of CEA for generously offering us the facilities of their laboratories.

instrument. While the pulseheight distribution in each of the individual counters T4 and T5 is quite broad, the value of E_c leads to a rather narrow distribution with the proper choice of α/β . The energy resolution for various energies is shown in fig. 9. Any choice of α and β which significantly changes the α/β ratio degrades this resolution.

The data from the calibration runs were subjected to the same tagging criteria as the flight data to determine the electron identification efficiency. The elimination of all events which trigger the guard counter G leads to a loss of about 10% of the electrons, and is nearly energy independent up to a few GeV. The requirement that the pulse height in counter T3 is close to the most probable energy loss of a minimum ionizing particle results in the loss of 10% of the electrons due

to the presence of a significant Landau tail and back-scattered electrons.

The ratios by which the various permissible tagging paths are followed by electrons are strongly energy dependent. Nevertheless, the total efficiency for electron detection is quite independent of energy. This efficiency is shown in fig. 10. The dip around 200 MeV occurs because incident electrons of this energy often produce pulse heights in T4, T5 and T6 which are all close to the minimum ionization peak, resulting in a rejection as a penetrating particle. The fact that the efficiency was determined directly by calibration experiments greatly enhances the reliability of the measurement of the electron energy spectrum.

It is a pleasure to acknowledge the leading role of Messrs. H. Boersma and W. Johnson in the design and the construction of the equipment as well as the execution of balloon flights and calibration measurements. We are greatly indebted to Messrs. Burdick, Hunsiger and Reisch for many contributions to the electronics and to Mr. Bonasera who designed and tested the ground station and the on-board tape recording device. Our thanks are due to Mr. R. Ekstrom for providing the computer program. Several stimulating discussions with Dr. D. Muller are gratefully acknowledged.

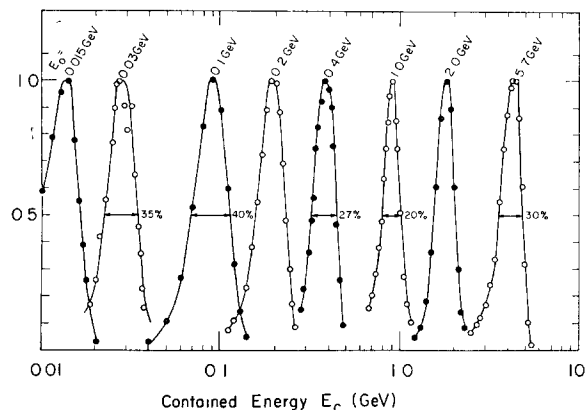


Fig. 9 The energy resolution of the detector system at various energies of incident electrons as obtained from accelerator exposures.

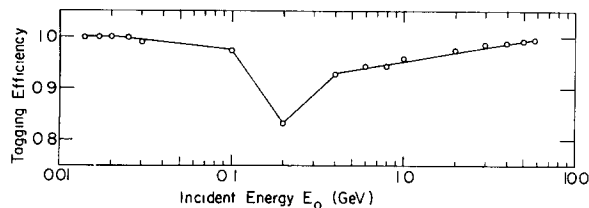


Fig. 10. The efficiency of the tagging procedure for electron detection as a function of incident electron energy E_0 obtained from accelerator exposures.

References

- 1) D. Hovestadt, P. Meyer and P. J. Schmidt, to be published.
- 2) D. Hovestadt and P. Meyer, Proc. 11th Intern. Conf. *Cosmic rays* (Budapest, 1969).
- 3) J. V. Jelley, *Cerenkov radiation* (Pergamon Press, London, 1958).
- 4) M. Gardner, D. G. Jones, F. E. Taylor and A. W. Wolfendale, Proc. Phys. Soc. **80** (1962) 697.
- 5) W. H. Barkas and H. Berger, Nucl. Sci. Ser. **39** (Nat. Acad. Sci., NRC, Washington, 1964).
- 6) P. Trower, High energy particle data, UCRL Report 2426, vol. II (1966).
- 7) K. Ott, Z. Naturforsch. **9a** (1954) 488.
- 8) H. H. Nagel, Z. Physik **186** (1965) 319.
- 9) U. Volkel, DESY Report 65/6 (1965);
U. Volkel, DESY Report 67/16 (1967).
- 10) A. Kantz and R. Hofstadter, Nucleonics **12**, no. 3 (1954) 36.
- 11) H. Burfeindt, DESY Report 67/24 (1967).
- 12) H. Lengeler, W. Tejessy and M. Deutschmann, Z. Physik **175** (1964) 283.
- 13) B. Rossi, *High energy particles* (Prentice Hall, Englewood Cliffs, N.J., 1952).
- 14) J. L. Fanselow and R. C. Hartman, private communication.
- 15) R. W. Williams, Rev. Mod. Phys. **36** (1964) 815.